

Centrifuge modelling of pile-soil interaction in liquefiable slopes

Stuart K. Haigh* and S.P. Gopal Madabhushi

Cambridge University, Department of Engineering, Trumpington St, Cambridge, UK

(Received May 22, 2009, Accepted December 22, 2010)

Abstract. Piles passing through sloping liquefiable deposits are prone to lateral loading if these deposits liquefy and flow during earthquakes. These lateral loads caused by the relative soil-pile movement will induce bending in the piles and may result in failure of the piles or excessive pile-head displacement. Whilst the weak nature of the flowing liquefied soil would suggest that only small loads would be exerted on the piles, it is known from case histories that piles do fail owing to the influence of laterally spreading soils. It will be shown, based on dynamic centrifuge test data, that dilatant behaviour of soil close to the pile is the major cause of these considerable transient lateral loads which are transferred to the pile. This paper reports the results of geotechnical centrifuge tests in which models of gently sloping liquefiable sand with pile foundations passing through them were subjected to earthquake excitation. The soil close to the pile was instrumented with pore-pressure transducers and contact stress cells in order to monitor the interaction between soil and pile and to track the soil stress state both upslope and downslope of the pile. The presence of instrumentation measuring pore-pressure and lateral stress close to the pile in the research described in this paper gives the opportunity to better study the soil stress state close to the pile and to compare the loads measured as being applied to the piles by the laterally spreading soils with those suggested by the JRA design code. This test data shows that lateral stresses much greater than one might expect from calculations based on the residual strength of liquefied soil may be applied to piles in flowing liquefied slopes owing to the dilative behaviour of the liquefied soil. It is shown at least for the particular geometry studied that the current JRA design code can be un-conservative by a factor of three for these dilation-affected transient lateral loads.

Keywords: dilation; lateral spreading; pile-soil interaction; centrifuge modelling.

1. Introduction

The use of piles to carry structural loads through liquefiable strata to more competent ground is well established, but if the ground is sloping and hence susceptible to lateral spreading following liquefaction, the interaction between these piles and the surrounding flowing liquefied soil is still a subject of considerable research. It has been shown previously (e.g. Haigh *et al.* 2000) that even ground with slopes of as little as 3 degrees to the horizontal can suffer significant lateral spreads, whilst Abdoun *et al.* (2003) gave an insight into the overall behaviour of soil-pile systems, but the lack of instrumentation close to the piles means that the near-pile soil behaviour and its impact on

*Corresponding author, Ph.D., E-mail: skh20@cam.ac.uk

pile loading is still not well understood. The capacity of these lateral forces to cause damage to pile-founded structures has been dramatically illustrated in many of the earthquakes of the past forty years. One example of this is the failure of the Showa bridge during the 1964 Niigata earthquake, which is discussed in detail by Hamada (1992). The bridge was founded on 25 m long 300 mm diameter tubular steel piles passing through liquefiable soils on the bed of the Shinano river. When aerial photogrammetry was carried out after the earthquake, lateral spreads of up to 10 m were found to have occurred on the banks of the river. The flowing liquefied soil caused lateral loads on the piles resulting in the pier heads being deflected by approximately 1 m. This was sufficient for the bridge decks to be dislodged, as shown in Fig. 1.

Piles passing through laterally spreading deposits are generally designed using pseudo-static design methods, which apply a multiple of overburden stress as an applied lateral pressure. An example of this approach is documented in the Japanese Road Association highway bridges code (JRA 1996), which applies 30% of total overburden stress as a lateral pressure in the liquefiable layer.

This paper reports the results of geotechnical centrifuge tests in which models of gently sloping liquefiable sand with pile foundations passing through them were subjected to earthquake excitation, seepage parallel to the slope being maintained by pumping. In above-water field slopes in which liquefaction to the ground surface is expected owing to high water-tables, it might be expected that seepage parallel to the slope would be encountered; this influenced the use of pumping to maintain this seepage boundary condition.

The seepage condition was developed using peristaltic pumps to circulate pore-fluid from a tank

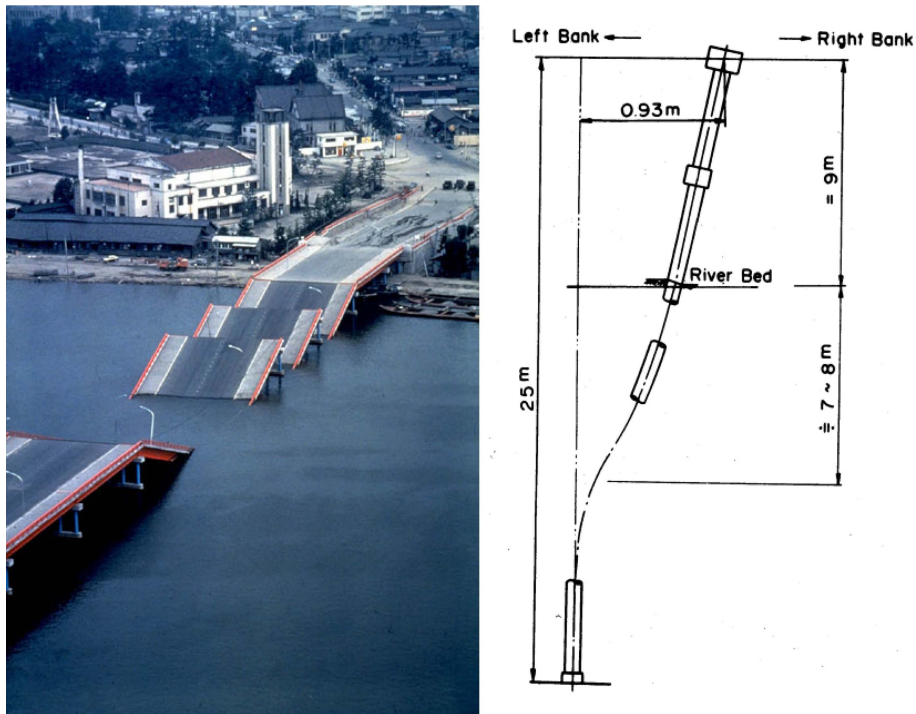


Fig. 1 The collapsed Showa bridge and one of its piles (after Hamada 1992)

into the drain at the head of the slope. Overflow pipes were present at the head and toe of the slope to maintain a constant water-table in these locations, with the oil collected from these overflows being re-circulated through the model to avoid extra weight having to be carried on the centrifuge package. Whilst the experiments described here did not measure the impact difference made by the presence or non-presence of seepage flow, it might be expected that downslope seepage forces might destabilise the slope resulting in higher magnitudes of lateral spread than would be the case with a fully submerged slope with no seepage flow.

The soil close to the pile was instrumented with pore-pressure transducers and contact stress cells in order to monitor the interaction between soil and pile and to track the soil stress state both upslope and downslope of the pile. Whilst dynamic centrifuge modelling of liquefaction-related phenomena such as lateral spreading are established techniques, researchers such as Abdoun *et al.* (2003) and Dobry *et al.* (2003) at RPI and Boulanger *et al.* (2003) at UC Davis also having investigated the effects of lateral spreading on pile foundations, instrumentation to measure the soil stress state has generally not been present close to the piles, research having focused on the bending moments induced in the pile by the flowing soil. The presence of instrumentation measuring pore-pressure and lateral stress close to the pile in the research described in this paper gives the opportunity to better study the soil stress state close to the pile and to compare the loads measured as being applied to the piles by the laterally spreading soils with those suggested by the JRA design code. Abdoun (1997) concluded from analysis of bending moment data that a lateral pressure of 9.5 kPa at all depths was applied to the pile by the liquefied soil. Further analysis of the same data by Dobry and Abdoun (1998) suggested that an inverse triangular pressure distribution falling from 17 kPa at the surface to zero at 6 m depth better fits the observed bending moments. Gonzalez *et al.* (2009) demonstrated with pore-pressure transducers close to piles in laterally spreading soil that sustained negative excess pore-pressures are generated close to piles during lateral spreading forming an inverted cone of dilating soil around the pile. The authors highlight the impact that this has in centrifuge models in which pore-fluid viscosity is not scaled, as the greater seepage velocity in water saturated models will more rapidly eliminate this zone of negative excess pore-pressure than would be the case in a prototype system. Dilation of soil around pile foundations has also been noted by researchers such as Brandenburg *et al.* (2007) but the use of water as a saturation fluid makes the excess pore-pressure data in these cases quantitatively unreliable, as dissipation of the pore pressures can occur even at the short timescales of centrifuge model earthquakes. Rollins *et al.* (2005) also measured dilation around a pile during the flow of liquefied soil during blast-induced lateral spreading. As earthquake-induced loading was not present, this induced monotonic dilation of the soil surrounding the pile and the true dynamic behaviour of the system was not investigated.

Although it can be seen that the piles of the Showa bridge had significant flexibility, the piles tested in the test series described here were very stiff relative to the soil. This will result in higher loads being exerted than would be the case if the piles were flexible. This high stiffness was chosen in order that a worst-case scenario could be investigated. Pile flexibility would have the effect of decreasing the applied pressures owing to the reduction in relative soil-pile movement.

2. Centrifuge model tests

Geotechnical centrifuge modelling is a technique by which the stresses and strains in a full-scale prototype can be recreated in a scale model. This condition is obviously necessary for true prototype

Table 1 Centrifuge scaling laws

Parameter	Model/prototype	Dimensions
Length	1/N	L
Acceleration	N	LT ⁻²
Velocity	1	LT ⁻¹
Strain	1	1
Stress	1	ML ⁻¹ T ⁻²
Force	1/N ²	MLT ⁻²
Mass	1/N ³	M
Seepage velocity	N	LT ⁻¹
Time (seepage)	1/N ² (1/N using viscous pore fluid)	T
Time (dynamic)	1/N	T
Force	1/N ²	MLT ⁻²

behaviour to be observed from a scale model owing to the non-linearity of soil constitutive behaviour. The principles of centrifuge modelling and the scaling laws required for homology of stresses and strains to apply are discussed in detail by Schofield (1980 and 1981). The technique offers considerable practical and economic advantages over field testing for “static” problems, but the argument becomes even more persuasive when considering dynamic earthquake loading. The unpredictability of the timing of earthquake events makes the monitoring of field structures during earthquakes both expensive and unreliable owing to the problems of maintaining complex instrumentation in the expectation of a future large magnitude earthquake event that might take several decades to occur.

Centrifuge modelling also allows the investigation of the behaviour of structures which are “designed to fail”, allowing the development of failure mechanisms to be investigated. This is obviously not possible with instrumented field structures whose value is such that their failure must be prevented. Dynamic centrifuge modelling offers a relatively inexpensive method of obtaining high-quality data from dynamic soil-structure interaction problems in the controlled environment of the geotechnical laboratory.

In the coming sections, all parameters will be discussed at their equivalent prototype values, conversion between these and the actual model parameters being by way of the scaling laws summarised in Table 1 and discussed by Schofield (1980 and 1981).

2.1 Test series

A series of dynamic centrifuge tests were carried out at Cambridge University using the SAM earthquake actuator described by Madabhushi *et al.* (1998) on the 10 m beam centrifuge. The tests will be briefly described here, but a more detailed explanation is available in Haigh (2002).

The test geometry is as shown in Fig. 2, with dimensions at model scale. The test was carried out at 50g, so all dimensions should be scaled up by a factor of 50 to achieve prototype dimensions. The tests consisted of a 6 m thick gently sloping medium-dense liquefiable layer, (relative density 50%) with a slope angle of approximately 6 degrees overlying a triangular dense sand base layer, (Relative density 80%). Two brass model piles with square and circular cross sections were present within the slope in order to quantify the effects of pile shape on the applied lateral loads. In this

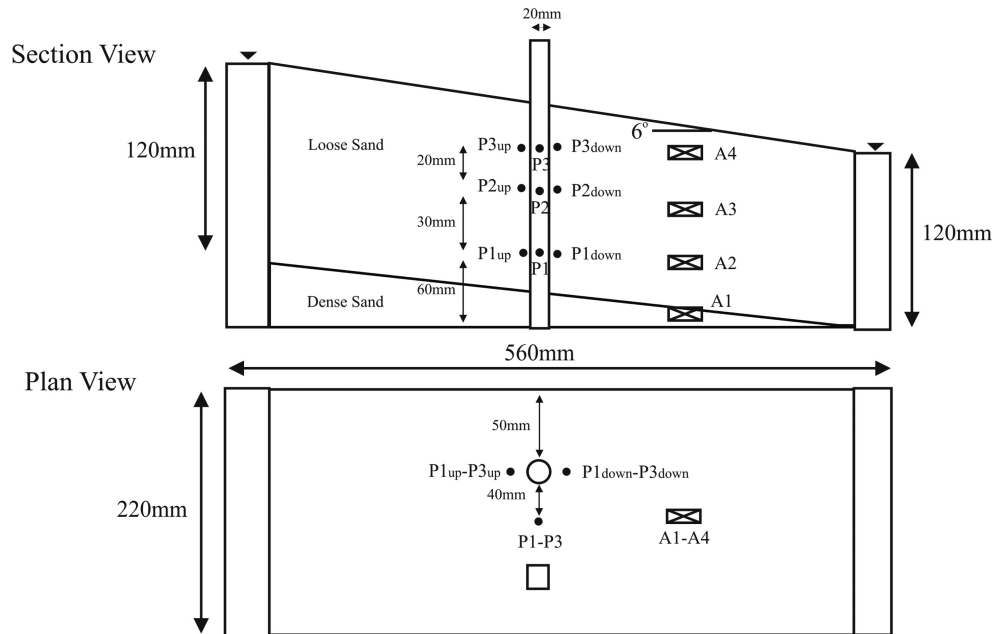


Fig. 2 Centrifuge model geometry (dimensions at model scale)

paper only the behaviour of the circular pile will be discussed in detail, as little difference in results was observed between the two pile profiles. The global behaviour of square and circular piles was found to be very similar, with the same behaviour being observed upslope and downslope of both piles. Square section piles attracted approximately 8% more loading than circular piles with the same frontal area. This matches very closely with the value of approximately 11% which can be calculated based on upper and lower bound mechanisms for square and circular bodies being displaced through cohesive media. For a circular body the resistance is between 9.14 (Randolph and Houlsby 1984) and $9.42 C_u$ (Salençon 2001) and for a square body between 10.28 and $10.8 C_u$.

The model was prepared by air pluviation, with the rate of pouring and hopper height being controlled in order to achieve the desired sand density. The sand used was fraction E silica sand with properties as summarised in Table 2. Reservoirs of coarser fraction B silica sand whose properties are also given in Table 2 were present at the top and bottom of the slope in order to achieve a plane-strain seepage condition. Silicone oil with a viscosity of 50 cSt was used as pore-fluid in order to correct the anomaly between seepage and dynamic time, as shown in Table 1. This was pumped into the reservoir at the top of the slope throughout the tests in order to maintain the sloping water-table with seepage flow parallel to the slope.

The sand was pluviated with the model pile already in place, the installation effects of the pile not being modelled. In the prototype it might be expected that the soil around the pile would be densified during pile driving, possibly resulting in a less liquefiable region around the pile. In contrast, pile boring may loosen the soil surrounding the pile. These effects were, however, not modelled in the work described here.

The model was contained within an Equivalent Shear Beam (ESB) model container designed to have identical stiffness to the soil contained within it in order to minimise the reflection of stress

Table 2 Properties of fraction B & E silica sand

Property	Value	Value
ϕ_{crit}	36°	32°
D_{10}	0.84 mm	0.095 mm
D_{50}	0.9 mm	0.14 mm
D_{60}	1.07 mm	0.15 mm
e_{min}	0.495	0.613
e_{max}	0.82	1.014
G_s	2.65	2.65

waves from the ends of the box. As the soil liquefies the soil stiffness falls whereas the box stiffness remains identical. These effects have been examined by Teymur (2003) who showed that the effects of the end-walls on soil behaviour in the central third of the box were negligible.

The model piles were constructed of brass with a prototype diameter of 1 m and hence a very high prototype bending stiffness of approximately 4.5 GNm^2 . This would correspond to a 1 m diameter steel pile with a wall thickness of 65 mm. The model pile foundations were clamped to the base of the model container in order to simulate the deep embedment of the prototype piles into an underlying competent stratum in the field. A typical pile of 1m diameter would have a wall thickness of approximately 10 mm, making these piles approximately six times stiffer than might be typical. This was a deliberate choice to minimise the effects of pile flexibility on the recorded data, thus measuring conservative values of applied stresses that could be used in design. The choice of an essentially rigid pile also removes many of the complexities of the interaction between a flexible pile and flexible soil, allowing the data recorded in these experiments to be more easily interpreted.

The instrumentation used included Druck PDCR81 pore-pressure transducers (PPTs), D.J. Birchall type A23 accelerometers and Entran EPL series total stress cells with a 700 kPa range. The accelerometers and PPTs were calibrated using standard techniques, but in order to confirm the suitability of the stress cells for measuring earth pressures these were calibrated with fluid and also with soil in a separate centrifuge test. The calibrations were shown to be both linear and identical, giving a high degree of confidence in the use of these instruments in these tests. This confirms the results of Dewoolkar *et al.* (1998) who also obtained good results using these gauges in saturated sands.

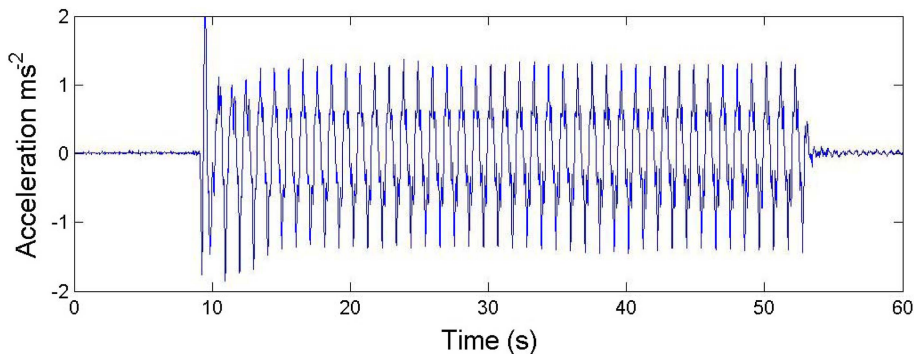


Fig. 3 Centrifuge input motion

The model was subjected to a g -level of 50 g in a centrifuge and saturated with 50 cSt silicone oil using peristaltic pumps until a steady-state seepage regime was achieved. This viscous pore fluid is used in order to correct the inconsistency between the scaling laws for seepage and dynamic velocities that occur if water is used as pore fluid, as discussed by Schofield (1981). The model was then subjected to an approximately sinusoidal earthquake with a peak acceleration of 20% of g at the model base, a frequency of 1Hz and a duration of 45 s, as shown in Fig. 3, and time histories of acceleration, pore pressure and contact stress were measured at a variety of points within the model.

3. Results

3.1 Far-field behaviour

The slope was observed to displace by 1.5 m at the surface during the earthquake and during dissipation of pore pressures. The behaviour of soil in the far-field is as illustrated by the pore-pressure and acceleration time histories shown in Figs. 4 and 5 respectively. It can be seen from Fig. 4 that as the model is subjected to base shaking, pore pressures in the liquefiable soil build up rapidly to a value consistent with full liquefaction, then remain at this elevated value until the end of the earthquake. The pore-pressures measured in the soil slope show a limited degree of cyclic behaviour, with “shock-waves” of dilative behaviour travelling vertically upwards through the model as a pulse of acceleration causes the stress path of the loose contractive soil to cross the characteristic state line causing dilation. This dilative shock-wave begins when the base moves in a downslope direction, exerting the maximum shear stress in the liquefied soil as static and dynamic shear stresses are in the same direction. These shock waves have previously been observed by Kutter and Balakrishnan (1999). The acceleration and pore-pressure shock waves can be shown to

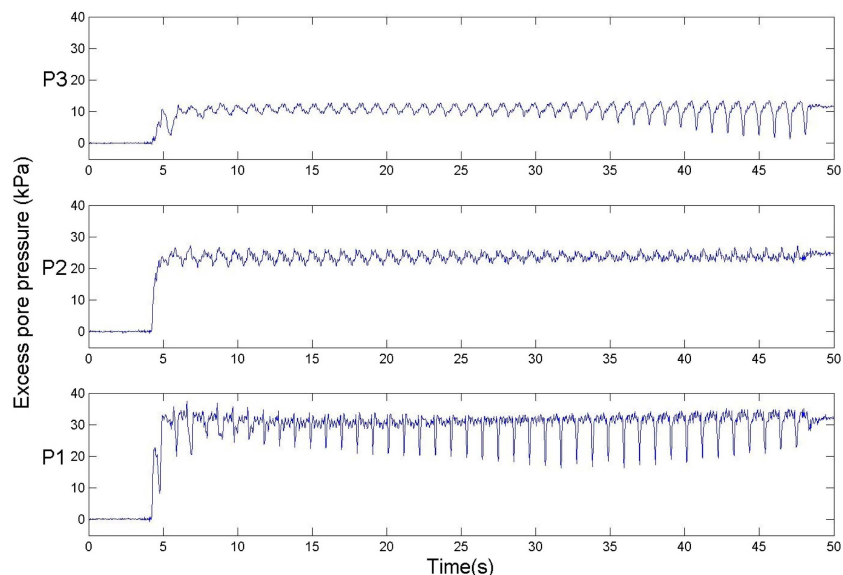


Fig. 4 Free-field pore-pressures measured in centrifuge model

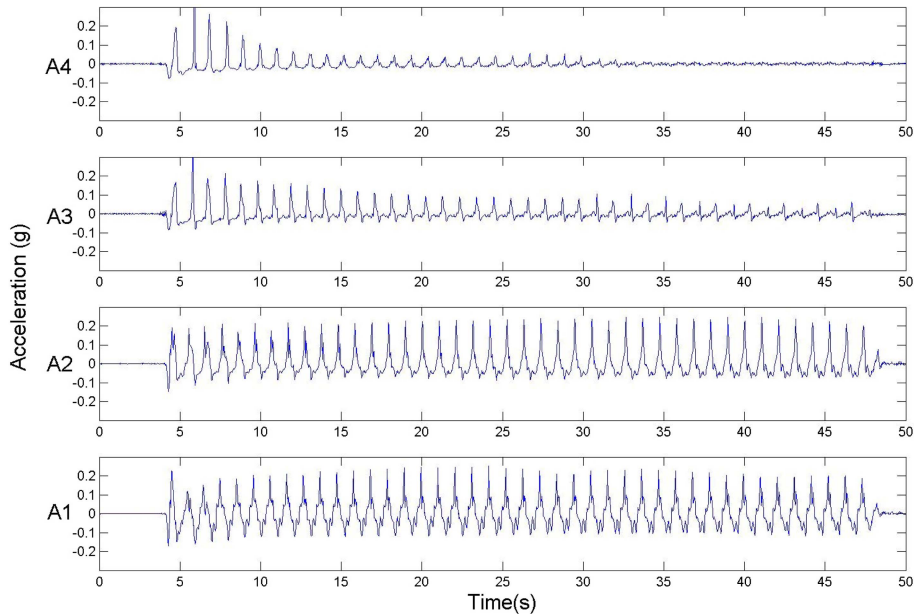


Fig. 5 Free-field accelerations measured in centrifuge model

both have a velocity of approximately 10 m/s, consistent with the results of Kutter and Wilson (1999) and indicating a shear stiffness for the liquefied soil of 200 kPa. Whilst conventional wisdom suggests that at full liquefaction soil has zero shear stiffness, the passage of the shear wave through the soil causes pore-pressures to drop as the soil attempts to dilate. This allows the shear wave to pass through the soil as a dilative shock wave, with the soil having a significant apparent shear stiffness.

From Fig. 5 it can be seen that this build-up of pore-pressure and hence drop in effective stress results in a progressive attenuation of the accelerations measured close to the soil surface. The accelerations measured within the soil such as A4 also become more asymmetric compared with that imparted at the base (A1). This is due to the spikes of acceleration that occur in an upslope direction when the shock-wave passes and the soil dilates, forcing the soil that was previously flowing downslope to comply with the imparted base motion and to accelerate in an upslope direction. This aspect was described in detail by Haigh *et al.* (2001) in which the behaviour was compared with that predicted by an effective stress based Newmarkian sliding block model.

3.2 Near-pile behaviour

In order to measure the near-pile soil stress state, pore-pressure transducers were placed approximately 0.5 m upslope and downslope of the pile at depths of 2 m and 3.5 m. These were supplemented by contact stress cells attached to the upslope and downslope faces of the pile at the same depths. This instrumentation allows us to gain an insight into the stress path behaviour of soil elements close to the faces of the pile. The presence of instrumentation close to the pile may affect the behaviour measured. This is a paradigm that affects all measurements, in this case the impact being minimised by the use of miniature transducers, the PPTs having a diameter of 5 mm and a

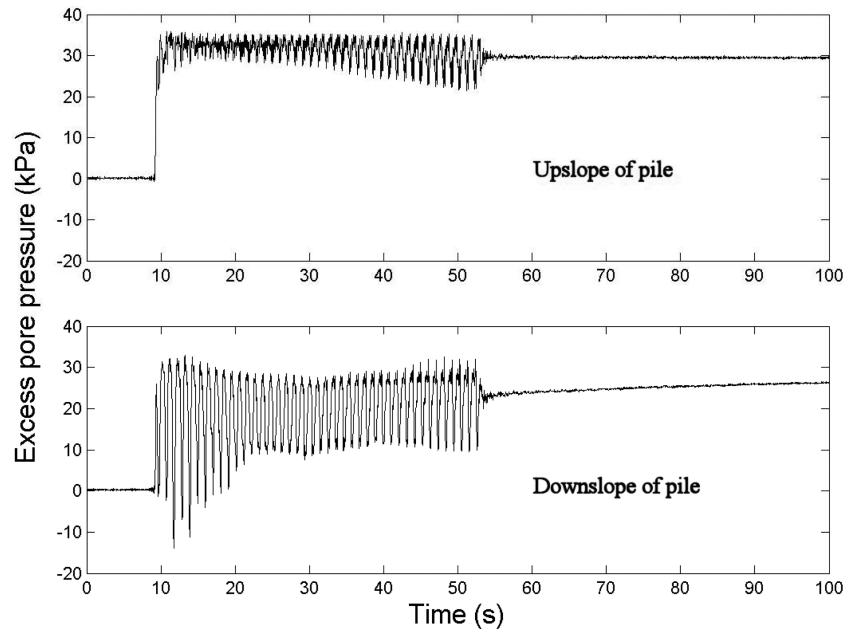


Fig. 6 Near-pile excess pore-pressures at 3.5 m depth

length of 10 mm. Due to the downslope flow of soil during the lateral spreading, the position of these PPTs altered slightly during the earthquake. Post-earthquake excavation of the model revealed that the PPTs downslope of the pile had moved approximately 1m further from the pile than their initial position, doubling their distance from the pile. The PPTs upslope of the pile had not moved significantly, as the zone of soil upslope of the pile was restrained in its movement by the presence of the pile.

The excess pore-pressures measured close to the pile at 3.5 m depth are as shown in Fig. 6. It can be seen from the pore-pressure time-histories that very different soil behaviour occurs upslope and downslope of the pile. Specifically, significant dilatant behaviour occurs downslope of the pile, pore-pressures of -45 kPa relative to the fully liquefied pore pressure (-15 kPa relative to hydrostatic values) being measured. This results in a net force on the pile acting in the downslope direction from fluid pressure alone, in addition to any net downslope pressure due to differences in the effective stress in the soil. The time history of this hydrodynamic force can be seen in Fig. 7. Using the face area of the pile and assuming a triangular variation of pore pressure with depth, the peak hydrodynamic force acting on the pile can be shown to be 250 kN.

The figure shows a maximum pressure difference of 50 kPa being applied to the pile at this depth, mostly resulting from the large dilatant suction spikes observed in the time history of pore pressure downslope of the pile. Post-earthquake, a 10 kPa pore pressure differential exists which falls as excess pore-pressures dissipate to the initial value of 3 kPa. This 3 kPa value corresponds closely to the 2 kPa difference predicted from the slope of the soil surface, there being a 0.2 m drop in sand height between the transducer positions.

It is obvious that the sand near to the downslope face of the pile is showing much more dilatant behaviour than that immediately upslope of the pile. The reason for this can be seen by looking at the stress path behaviour of the soil elements. This behaviour has also been observed in full-scale

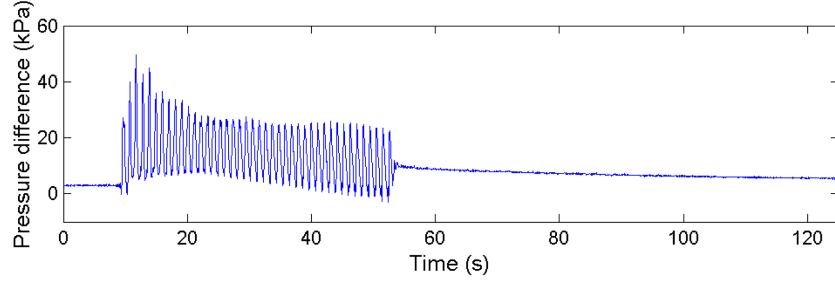


Fig. 7 Net hydrodynamic pressure in the downslope direction on pile at 3.5 m depth

tests by Suzuki *et al.* (2005) who carried out shaking table tests on pile-soil interaction in both level ground and in slightly sloping ground. The authors observed that significant pore-water pressure reduction was observed downslope of the pile resulting in the pile being pulled downslope.

3.3 Analysis of data

The initial stress state of elements both upslope and downslope of the pile (assuming shear stresses to be negligible for gentle slopes and hence principle stress directions to be vertical and horizontal) is as shown in Fig. 8(a), with mean effective confining stress p' and deviatoric stress q given by Eqs. (1) to (3).

$$K_0 = \frac{\sigma'_H}{\sigma'_v} \quad (1)$$

$$p'_{static} = \frac{(1 + 2K_0)(\sigma'_v - u_{static})}{3} \quad (2)$$

$$q_{static} = (1 - K_0)(\sigma'_v - u_{static}) \quad (3)$$

If one considers a soil element downslope of the pile, the stress path behaviour during flow (ignoring any dynamic effects) could be considered equivalent to a relaxation of the horizontal total

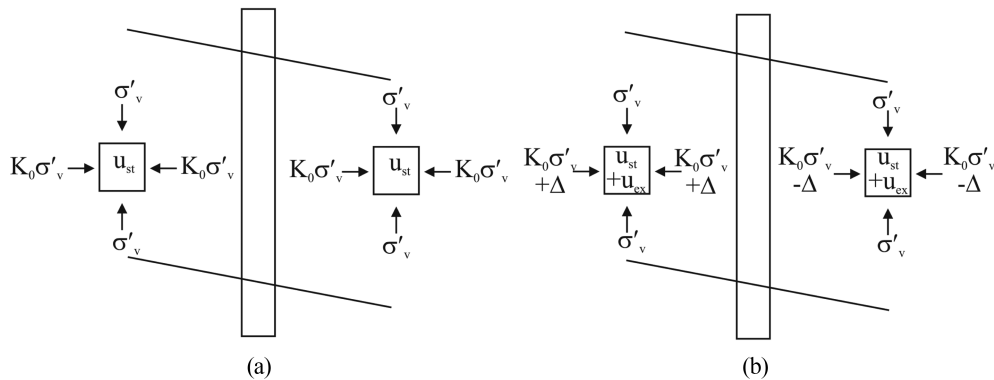


Fig. 8 Soil total-stress states before and during flow (Δ is the assumed horizontal stress change)

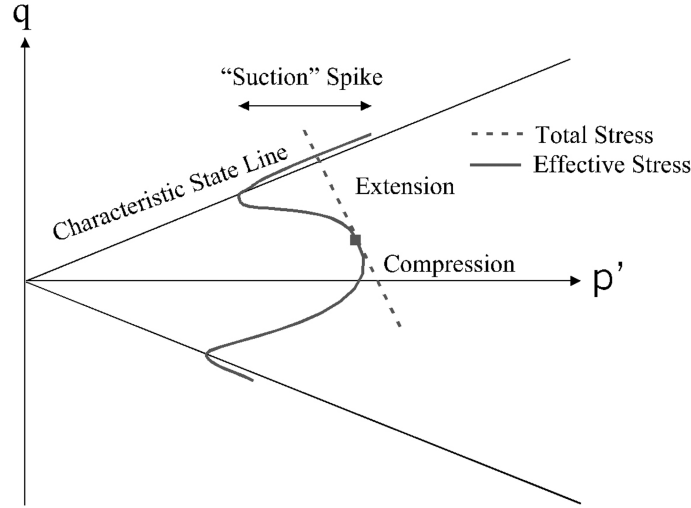


Fig. 9 Total and effective stress paths in horizontal extension and compression

stress acting on the soil element as the far-field soil moves downslope away from the pile, with vertical and transverse (perpendicular to the shaking direction) total stresses assumed to remain constant. The variation of the transverse total stress is not measured in this case, so some assumption has to be made. Upslope of the pile soil is moving towards the pile and failure is induced by increasing the horizontal total stress on the element as is shown in Fig. 8(b). These total stress paths are shown by the dashed line in Fig. 9, with the equations for p' and q given in Eqs. (4) and (5), where Δ is the assumed horizontal stress change.

$$p'_{down} = p'_{static} - \frac{\Delta}{3} - u_{excess} \quad q_{down} = q_{static} + \Delta \quad (4)$$

$$p'_{up} = p'_{static} + \frac{\Delta}{3} - u_{excess} \quad q_{up} = q_{static} - \Delta \quad (5)$$

Considering these stress paths within the characteristic state framework derived by Luong & Sidaner (1981) requires definition of characteristic state lines (CSLs) separating regimes in which soil contracts on shearing between the lines, termed the subcharacteristic regime, from those regimes in which the soil dilates on shearing or the surcharacteristic regime. (This framework is similar to that described by Ishihara *et al.* (1975) in which the characteristic state line is instead referred to as a phase transformation line.

If we assume that the characteristic state line follows the equation $q = Mp'$; as q_{static} is positive if K_0 is less than unity, for the soil element to approach the characteristic state line by increasing the horizontal stress (in a fully drained test) q must change by $(Mp' + q_{static})$ to hit the CSL at $q = -Mp'$ and exhibit passive failure. For failure by decreasing the horizontal stress, q must increase by the smaller value $(Mp' - q_{static})$ to hit the CSL at $q = Mp'$ and exhibit active failure. The initial positive value of q thus gives dilative behaviour at a lower stress change in horizontal extension than in horizontal compression, assuming the CSL to have similar slopes in extension and compression.

The tests described here are obviously not fully drained but this argument still holds true for

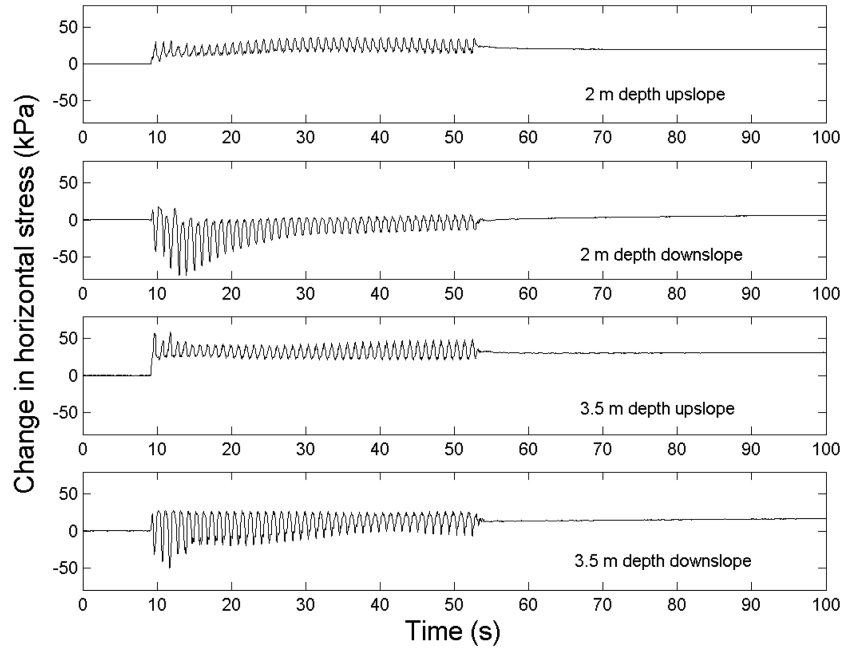


Fig. 10 Changes in lateral stress measured on faces of pile

undrained tests. The undrained test paths, showing the generation of positive and negative pore pressures are shown by the solid line in Fig. 9. Excess pore pressures are given by the difference between total and effective stress paths, and show small amounts of dilation in the compressive test and large amounts in the extensile test, in which event suctions relative to the initial hydrostatic

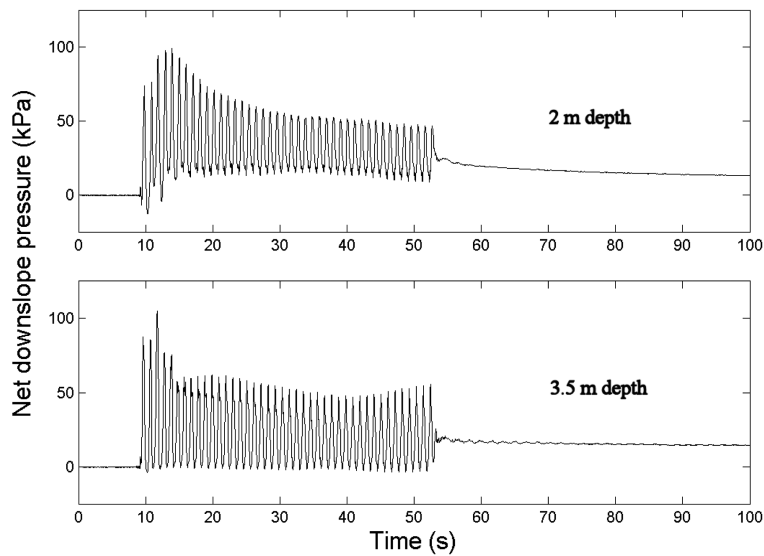


Fig. 11 Net earth-pressures in the downslope direction measured on pile

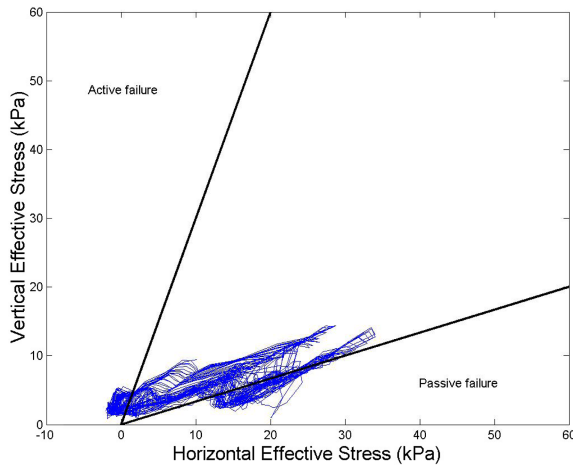


Fig. 12 Stress path upslope of the pile during earthquake at 3.5 m depth

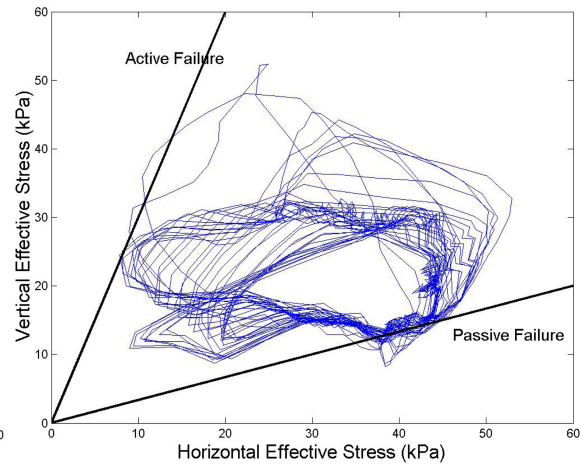


Fig. 13 Stress path downslope of the pile during earthquake at 3.5 m depth

pressures are eventually generated. This is exactly the behaviour observed from the centrifuge test data.

The horizontal stresses measured on the faces of the pile are shown in Fig. 10, with the resultant pressure in the downslope direction being shown in Fig. 11. It can be seen that large transient loads are applied to the pile in the downslope direction, with peak values of approximately 110 kPa being measured.

As the horizontal stresses on the faces of the pile are measured during the tests at the same locations as pore-pressure data, this allows effective stress-paths to be plotted. It is assumed that the vertical total stress remains constant at γz (where z is the depth of the transducer below the soil surface) so vertical effective stress is $\sigma'_v = \gamma z - u$ whereas horizontal effective stress is $\sigma'_H = \sigma_H - u$. These stress paths are shown for elements immediately upslope and downslope of the pile in Figs. 12 and 13. It can be seen from Fig. 12 that upslope of the pile the stress path cycles up and down the passive failure line, as might be expected as soil is continuously being pushed down the slope onto the pile causing the soil to fail. Downslope of the pile, it can be seen from Fig. 13 that failure occurs in both active and passive failure envelopes at some points, though this stress path is much less stable with time due to the pore-pressure transducer moving away from the pile with the flowing soil. Post-test excavation revealed that the PPT had migrated away from the pile by 0.5 m with the flowing soil, doubling its distance from the pile surface.

3.4 Implications to practice

One of few design codes to give guidance for the design of piles in laterally spreading soils is the Japan Road Association's Highway Bridges code (1996). This suggests designing for passive pressure in any non-liquefied surface crust and a lateral pressure equal to 30% of the total overburden stress in the liquefied layer. In the experiment described here an unsaturated and hence non-liquefiable crust of 0.25 m thickness was present above the water table due to g-field curvature, so this would be equivalent to designing for pressures of 10 kPa and 20 kPa at 2 m and 3.5 m depth respectively. The measured peak loads at these depths were respectively 107 kPa and 105 kPa, the

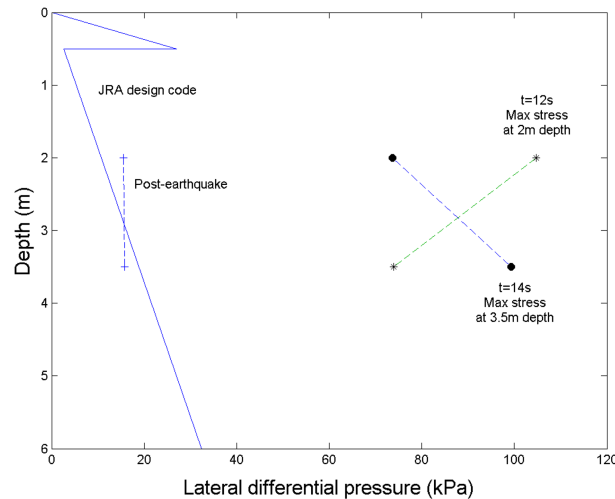


Fig. 14 Lateral loading measured on pile compared with design guidance from JRA

code hence underestimating peak transient loads by factors of 10 and 5 respectively, though the predicted values correlate much more closely with the post-earthquake residual loading, as shown in Fig. 14. The maxima of the pressures measured at the two depths do not occur simultaneously, that at 2 m depth occurring after 12s whereas that at 3.5 m depth occurs after 14s. Fig. 14 shows, however that at both of these time instants the measured lateral pressure at both of these depths significantly exceeds that suggested by the JRA design code.

It should also be noted that extra loading on the pile will result from frictional drag forces exerted by the soil on the sides of the pile, as well as the active and passive loading on the front and back faces. This loading will tend to result in increased downslope loading of the pile, but these forces were not measured in the experiments described here. The overall forces on the pile may thus be greater than those measured here.

These measurements imply that the peak transient bending moments that must be carried by a relatively rigid pile are significantly higher than those that would be designed for using the JRA code, exceeding design values by approximately a factor of 8. The residual post-earthquake values however fit relatively well with the design values. Wilson *et al.* (2000) compared lateral pressures on piles in liquefied level ground with those predicted by the American Petroleum Institute code (API 1993). He found that the lateral pressures even in level ground could exceed those predicted using a drained analysis by around 30%, but this becomes even more severe in sloping ground as dilatant soil is forced past the pile by the down-slope component of gravity.

In reality, all piles have some flexibility, which will affect the dynamic performance of the system. These effects can be grouped into two areas; firstly system flexibility will lower the forces attracted to the pile as the amount of dilation occurring next to the pile is related to relative pile-soil movement, which will be reduced by pile flexibility. Secondly, when significant pile deformation occurs, inertial effects will cause the bending moments not to be the double integral of the applied loading as the pile is not always in static equilibrium. This effect will tend to reduce the bending moments that must be carried by the pile, as the acceleration of the pile will tend to be in the same direction as the applied loading from the flowing soil. The quantification of these phenomena and their implications to pile design is discussed by Haigh and Madabhushi (2005).

4. Conclusions

A dynamic centrifuge model study has been carried out to investigate the interaction of pile foundations with laterally spreading ground. The lateral loads exerted on piles by laterally spreading soils have caused significant numbers of pile failures during past earthquakes in the past, and whilst research has been carried out in the past looking at the bending moments induced in the piles, little has been known about soil behaviour close to the pile. Novel features of these tests include the presence of dense instrumentation of the soil close to the pile in order to measure near field stresses and pore pressures. This has given a great deal of insight into the mechanics of the soil-pile interaction. The main conclusions of the study are as follows:

- (a) Dilation of liquefied soil is very important in determining the magnitude of the lateral loads induced on the pile. This especially occurs downslope of the pile where pore pressure drops of up to 40 kPa were observed.
- (b) Instrumentation of soil close to the pile has revealed that soil close to the upslope face of the pile maintains a state of passive failure throughout flow, whereas that on the downslope side of the pile oscillates between active and passive failure on alternate cycles of the earthquake.
- (c) Transient net pressures in a downslope direction of up to 110 kPa are imposed on the pile at 3.5 m depth, significantly more than those predicted by current design codes. The residual downslope pressures acting on the pile post-earthquake were approximately 20 kPa, comparable to those predicted by the Japanese highway bridges design code.

References

- Abdoun, T.H. (1997), "Modelling of seismically induced lateral spreading of multi-layered soil and its effect on pile foundations", PhD Thesis, Rensselaer Polytechnic Institute, Troy, NY.
- Abdoun, T.H., Dobry, R., O'Rourke, T.D. and Goh, S.H. (2003), "Pile response to lateral spreads: centrifuge modelling", *J. Geotech. Geoenviron. Eng.*, **129**(10), 869-878.
- American Petroleum Institute (API) (1993), "Recommended practice for planning, design and constructing fixed offshore platforms", API RP2A-WSD, 20th Ed. Washington DC.
- Brandenberg, S.J., Boulanger, R.W., Kutter, B.L. and Chang, D. (2007), "Liquefaction-induced softening of load transfer between pile groups and laterally spreading crusts", *J. Geotech. Geoenviron. Eng.*, **133**(1), 91-103.
- Dewoolkar, M.M., Ko, H.Y. and Pak, R.Y.S. (1998), "Suitability of total stress gages for soil pressure measurement", *Proc., Centrifuge '98*, Balkema, Rotterdam, **1**, 129-134.
- Dobry, R. and Abdoun, T. (1998), "Post triggering response of liquefied sand in the free field and near foundations", *Proc., 3rd ASCE Speciality Conf. on Geotechnical Engineering and Soil Dynamics - ASCE*, 270-300.
- Dobry, R., Abdoun, T., O'Rourke, T.D. and Goh, S.H. (2003), "Single piles in lateral spreads: field bending moment evaluation", *J. Geotech. Geoenviron. Eng.*, **129**(10), 879-889.
- Gonzalez, L., Abdoun, T. and Dobry, R. (2009), "Effect of soil permeability on centrifuge modeling of pile response to lateral spreading", *J. Geotech. Geoenviron. Eng.*, **135**(1), 62-73.
- Haigh, S.K., Madabhushi, S.P.G., Soga, K., Taji, Y. and Shamoto, Y. (2000), "Lateral spreading during centrifuge model earthquakes", *Proc., Int. Conf. GeoEng2000*.
- Haigh, S.K., Madabhushi, S.P.G., Soga, K., Taji, Y. and Shamoto, Y. (2001), "Newmarkian analysis of liquefied flow in centrifuge model earthquakes", *Proc., 4th Int. Conf. Recent Advances in Geotechnical Earthquake Engineering and Soil Dynamics*.
- Haigh, S.K. (2002), "Effects of liquefaction on pile foundations in sloping ground", PhD Thesis, Cambridge University, UK.

- Haigh, S.K. and Madabhushi, S.P.G. (2005), "The effect of pile flexibility on pile-soil interaction in laterally spreading ground", *Geotech. Spec. Public. - ASCE*, **145**, 24-37.
- Hamada, M. (1992), "Case studies of liquefaction and lifeline performance during past earthquakes", NCEER, NY.
- Ishihara, K., Tatsuoka, F. and Yasuda, S. (1975), "Undrained deformation and liquefaction of sand under cyclic stresses", *Soils Found.*, **30**(4), 73-89.
- Japan Road Association (1996), "Specifications for highway bridges, Part V: Seismic design", Japan Road Association, Tokyo.
- Kutter, B.L. and Balakrishnan, A. (1999), "Visualization of soil behavior from dynamic centrifuge model tests", *Proc., 2nd Int. Conf. on Earthquake Geotechnical Engineering*, Balkema, Rotterdam, **3**, 857-862.
- Kutter, B.L. and Wilson, D.W. (1999), "De-liquefaction shock waves", *Proc., 7th US-Japan Workshop on Earthquake Resistant Design of Lifeline Facilities and Countermeasures Against Soil Liquefaction*, NCEER, NY, 295-309.
- Luong and Sidaner (1981), "Undrained behaviour of cohesionless soils under cyclic and transient loading", *Proc. Int. Conf. Recent Advances in Geotechnical Earthquake Engineering and Soil Dynamics*, University of Missouri-Rolla, **1**, 215-220.
- Madabhushi, S.P.G., Schofield, A.N. and Lesley, S. (1998), "A new stored angular momentum based earthquake actuator", *Proc., Centrifuge '98*, Balkema, Rotterdam, **1**, 111-116.
- Randolph, M.F. and Houlsby, G.T. (1984), "The limiting pressure on a circular pile loaded laterally in cohesive soil", *Géotechnique*, **34**(4), 613-623.
- Rollins, K.M., Gerber, T.M., Lane, J.D. and Ashford, S.A. (2005), "Lateral resistance of a full-scale pile group in liquefied sand", *J. Geotech. Geoenviron. Eng.*, **131**(1), 115-125.
- Salençon, J. (2001), "Action d'une conduite circulaire sur unsold cohérent", *Proc., 15th International Conference on Soil Mechanics and Geotechnical Engineering*, Balkema, Rotterdam, **2**, 1311-1314.
- Schofield, A.N. (1980), "Cambridge geotechnical centrifuge operations", *Géotechnique*, **25**(4), 743-761.
- Schofield, A.N. (1981), "Dynamic and earthquake geotechnical centrifuge modelling", *Proc., Int. Conf. on Recent Advances in Geotechnical Earthquake Engineering and Soil Dynamics*, University of Missouri-Rolla, **3**, 1081-1100.
- Suzuki, H., Tokimatsu, K., Sato, M. and Abe, A. (2005), "Factor affecting horizontal subgrade reaction of piles during soil liquefaction and lateral spreading", *Seismic Performance and Simulation of Pile Foundations in Liquefied and Laterally Spreading Ground*, *Geotech. Spec. Public. - ASCE*, **145**, 1-10.
- Teymur, B. (2003), "Experimental study of boundary effects in dynamic centrifuge modelling", *Géotechnique*, **53**(7), 655-663.
- Wilson, D.W., Boulanger, R.W. and Kutter, B.L. (2000), "Observed seismic lateral resistance of liquefying sand", *J. Geotech. Geoenviron. Eng.*, **126**(10), 898-906.